JOURNAL GEOLOGICAL SOCIETY OF INDIA
Vol.73, May 2009, pp.697-714

Petrogenesis of the Bondla Layered Mafic-Ultramafic Complex, Usgaon, Goa

A.G. Dessai[1], D. B. Arolkar[1], D. French,[2] A. Viegas[1] and T. A. Viswanath[1]
[1]Department of Earth Science, Goa University, Taleigao Plateau, Goa 403 206, India
[2]Energy Technology, CSIRO, New Illawarra Road, Lucas Heights, New South Wales, Australia

Abstract The Bondla mafic-ultramafic complex is a layered intrusion that consists predominantly of peridotites and gabbronorites. A chromitite-pyroxenite-troctolite horizon serves as a marker to subdivide the intrusion into two zones. The Lower Zone displays gravity stratified layers of chromite that alternate with those of olivine, which up-section are followed by olivine+pyroxene-chromite cumulates. The Upper Zone comprises gabbroic rocks that exhibit uniform layering. On the basis of modal and cryptic variation exhibited by the minerals this zone can be subdivided in to several lithohorizons starting from the troctolites at the base to gabbronorites and leucogabbros at the top. The junction between the two zones is marked by the distinct reversal in cryptic variation exhibited by the chromites and pyroxenes.

The peridotite chromites contain higher Al_2O_3 and lower Cr_2O_3 than those from the chromitite above. Similarly clinopyroxenes from pyroxenite and troctolites are more magnesian that those from the peridotites stratigraphically below them. The complex in general is characterized by a gabbroic mineral assemblage in which both Ca-rich and Ca-poor pyroxenes coexist and displays a Fe-enrichment trend providing evidence of evolution from a contaminated tholeiitic magma. The rocks are characterized by low-TiO_2; Ni, Cr and V, show negative correlation with Zr whereas the large ion lithophile elements (LILE) are positively correlated and the Nb/La ratio varies from 0.4-0.6. These characteristics are consistent with a low-TiO_2 sub-alkaline tholeiitic magma that may have been modified by fractional crystallization and successive injections of more primitive melts in the magma chamber. The complex evolved in a periodically replenished magma chamber that consisted of two separate but interconnected sub-chambers.

Keywords: Layered complex, Peridotites, Gabbronorite, Chromitite, Cumulate, Goa.

INTRODUCTION

The coastal belt of Goa and adjoining parts of southern Maharashtra and northern Karnataka hosts at least five N-S trending mafic-ultramafic complexes which form a part of the Precambrian Goa-Shimoga schist belt. The Bondla mafic-ultramafic complex is one such intrusion in central Goa (Fig. 1) that hosts rich chromite deposits and is one of the potential occurrences for the platinum group mineralisation in western India. Except for the brief descriptions of sulphide mineralisation (Dessai et al. 1994; 1995 a) and the occurrence of chromites (e.g. Balakrishnan et al. 1992; Dessai et al. 1995 b), limited petrological information is available on this complex. PG mineralization in mafic – ultramafic complexes has also been described from Channagiri complex of the Shimoga schist belt (Alapieti et al. 1994; Devaraju et al. 1994; Vidyadharan and Palaniappan, 2006). We present a detailed account of the petrography, mineral-chemistry and whole rock geochemistry based upon which we classify this complex and discuss its petrogenesis.

REGIONAL GEOLOGY

The Bondla Complex is intrusive into greenstones of the western Dharwar craton (Fig. 1). The supracrustals consist of a volcanosedimentary assemblage that is dominated by metasediments with intercalations of metavolcanics. The metasediments consist of quartz-chlorite-sericite schists and phyllites with banded iron formations. These have been assigned to the Barcem Formation of the Goa Group (Gokul, 1985) that is correlated with the Chitradurga Group of the Dharwar Supergroup (late Archaean to early Proterozoic). The Goa Group rests on a basement of Anmod Ghat Trondhjemitic Gneiss that has yieded a Rb/Sr whole rock isochron age of 3400±140 Ma (Dhoundial et al. 1987) and is amongst the oldest gneiss

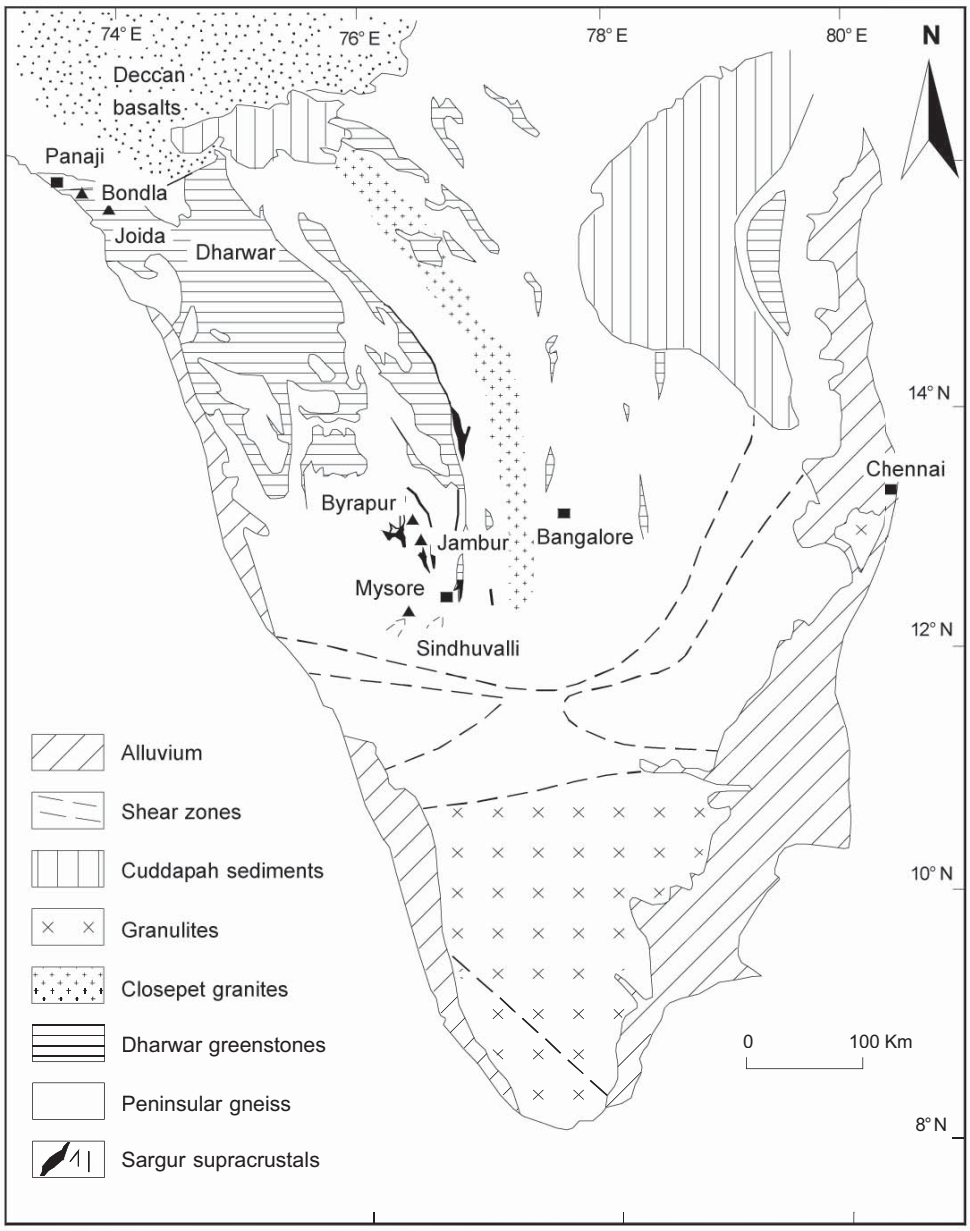

Fig.1. Regional distribution of layered complexes, southern India.

from the Dharwar craton. The greenstones are intruded by the syntectonic Chandranath Granite (Gokul and Srinivasan, 1976) which has been dated to 2650±100 Ma (Dhondial et al. 1987) by Rb/Sr method.

The Bondla complex occupies the axial region of a NW-SE trending anticline overturned towards the SW and is plunging NW by 20° (Dessai and Peshwa, 1982). A prominent shear zone (traceable on aerial photographs over 20 km NW-SE) expressed in the field by extensive crushing, brecciation and silicification approximately 1.5 km wide traverses the western limb of the fold and serves as the western boundary of the complex (Dessai et al. 1995). The rocks exhibit local deformation indicating that the complex was emplaced subsequent to major deformational episode coincident with the third phase of NW-SE trending folds (Gokul, 1985).

GEOLOGY OF THE BONDLA MAFIC-ULTRAMAFIC COMPLEX

The complex is exposed over a length of about 8 km (NW-SE) and extends from Ganje in the NW to Durgini in the SE (Fig. 2). In the western part peridotites/dunites and chromitites predominate whereas southeastwards e.g. at

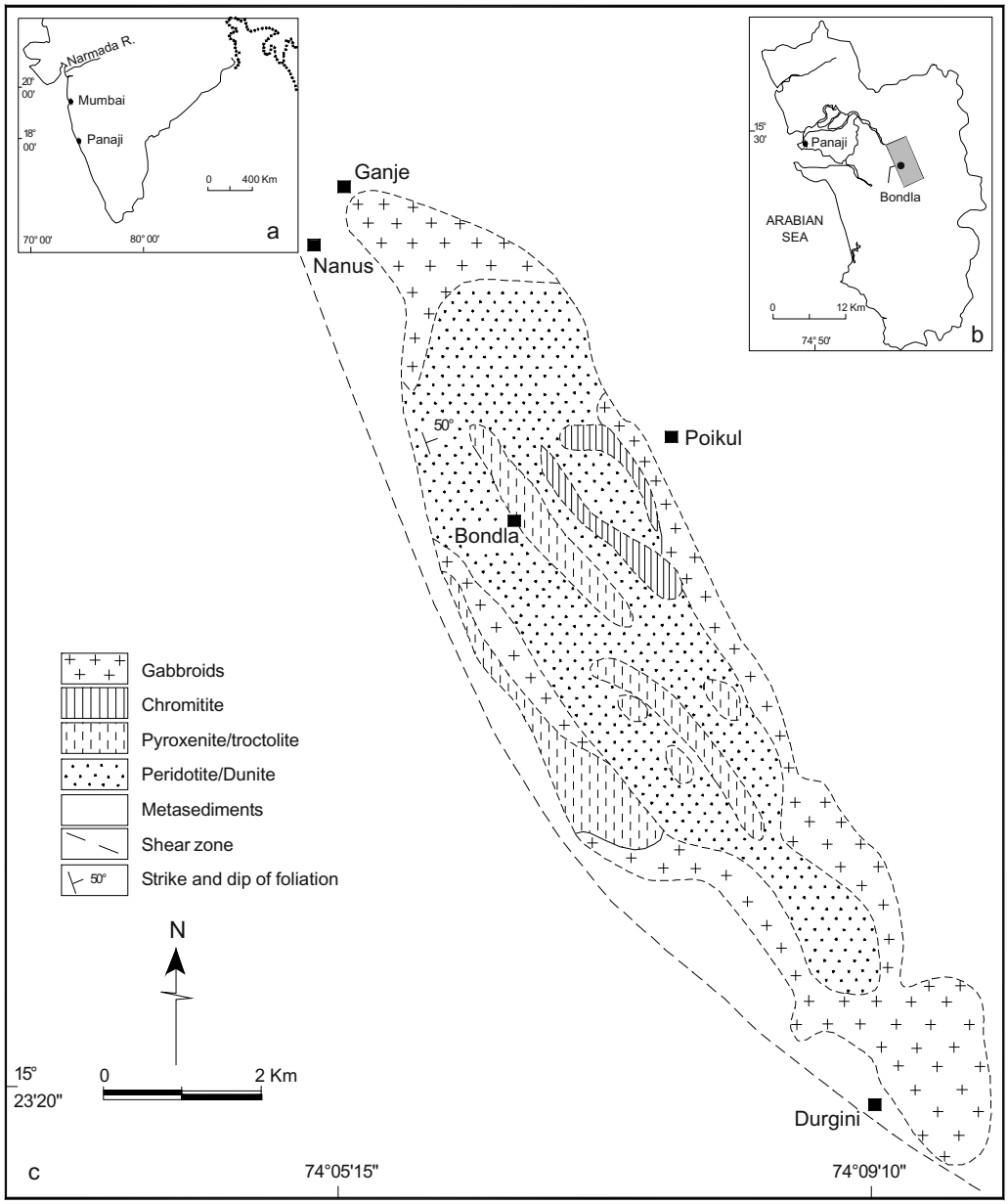

Fig.2. Location map of the study area. (**A**) Regional context (**B**) Area within Goa (**C**) Geological sketch map of the Bondla Mafic Ultramafic Complex with the localities mentioned in the text (partially modified after Balakrishnan et al. 1992).

Durgini, gabbroic rocks are preponderant. Layered gabbros are also exposed about 4 km SE of Durgini. These may possibly be extensions of the Bondla complex, however, due to thick laterite cover in the intervening areas their continuity cannot be ascertained beyond doubt. Hence they are not included in the present work.

The complex can be divided into two zones (following Wager and Brown, 1967) on the basis of incoming and outgoing of a specific cumulus mineral phase (dominance of lithologies). The Lower Zone exposed prominently at Nanus, Ganje and Poikul (4 km to the northeast of Bondla) has a thickness of about 900 m and is dominated by ultramafic rocks consisting of olivine and chromite cumulates. The Upper Zone which consists of cumulus pyroxene and plagioclase is about 600 m thick and is best exposed at Bondla and Durgini. The contact between the Upper and the Lower Zone is marked by a thick layer of chromitite that is overlain by a distinct but impersistent horizon of clinopyroxenite and troctolite. The latter has a thickness of about 200m and is exposed at the Bondla recreation park. The clinopyroxenite separates the mafic (clinopyroxene-plagioclase) cumulates above from the

ultramafic (olivine-chromite) cumulates below. On the basis of the spatial distribution of lithologies the complex consists of two distinct subdivisions the northwestern of ultramafic cumulates and the southeastern of mafic ones.

The Lower Zone at Nanus exhibits gravity stratified layers (Fig. 3) defined by olivine (3-10 cm) and chromite (1-5 rarely up to 10 cm). The layers are repetitive and show way up stratigraphy of chromite layers alternating with those of olivine. The lithological types constituting this zone are represented by dunite at the base followed by peridotite and chromitite. The harzburgite/wehrlite (peridotites) contains thin layers of chromite (0.5-5.0 cm) that alternate with

Fig.3. Chromite layering in peridotites, Bondla complex, Goa (scale bar: 2 cm).

olivine-rich (serpentinised) layers. They strike N 40° and dip 30° NE. In the vicinity of the shear zone the layers are sheared and fractured along which chromites have been remobilized forming a criss-cross pattern of chromite veins.

The top of the Lower Zone is marked by a thick horizon of chromitite which is best exposed at Poikul. It has a thickness of about 2.5 m and can be traced over 1.5 km. The chromitite is hard, massive and fine grained and consists of 80-90 vol % chromite the remainder being serpentinised olivine.

The chromitite is overlain by impersistent layers of clinopyroxenite which in turn is overlain by a prominent horizon of troctolite. Plagioclase makes its first appearance in troctolites which mark the beginning of the Upper Zone. Upsection the troctolite changes to a gabbronorite with the incoming of orthopyroxene and attains a thickness of about 230 m. In stratigraphically higher horizons the gabbronorite gives way to leucogabbros approximately 170m thick. This zone in general displays uniform layering (e.g. Wager and Brown, 1967). The modal compositions of the lithologies are presented in Table 1.

Table 1. Modal Composition (volume %) of rocks from the Bondla mafic-ultramafic complex

Sr No.	Smp. No.	Ol	Opx	Cpx	Opaq	Biot	Plag.
1	B22	81	1	-	17	-	-
2	B19A	72	-	11	16	-	-
3	N1	77	1	16	5	-	-
4	B15	26	-	-	74	-	-
5	B15A	20	-	-	80	-	-
6	B4	-	-	85	11	-	3
7	B14	0	-	83	12	-	4
8	BT 1	42	7	5	1	-	45
9	BT 2	33	4	1	Tr	-	61
10	GB 1	4	18	28	1	Tr	48
11	GB 2	Tr	16	31	2	Tr	49
12	GS 23		29	21	1	Tr	48
13	GS9	Tr	20	28	4	Tr	46
14	GS8	Tr	31	13	7	Tr	48
15	D12	3	18	29	2	Tr	46
16	D8	Tr	31	13	7	Tr	48
17	D11	7	20	29	1	Tr	42
18	G49	Tr	23	8	Tr	Tr	49
19	GD12	2	16	28	Tr	Tr	53
20	S35	3	16	19	2	2	58
21	S36	3	15	26	Tr	Tr	54
22	S40	4	13	15	3	Tr	64
23	S41	2	14	23	2	Tr	59
24	S39	4	11	16	2	Tr	66
25	S33	-	9	30	3	-	58
26	S22	3	22	14	2	Tr	58
27	S3	-	3	3	8	-	86

1: Dunite, 2-3: Peridotites, 4-5: Chromitites, 6-7: Pyroxenites
8-9: Troctolites, 10-18: Gabbronorites, 19-27: Leucogabbros

PETROGRAPHY AND COMPOSITION OF MINERALS

Mineral phases present in representative unaltered rock samples from the main lithologies were analyzed with an electron probe micro-analyzer, under standard conditions, at CSIRO, Australia, using natural and synthetic standards at an accelerating voltage of 15 kV and a specimen current of 3 nA. The width of the electron beam was 2-3 μm. A minimum of three spot were analyzed per mineral and average composition determined. At least four mineral grains were analyzed in each sample to characterize the amount of the intergrain variation. A total of 96 microprobe analyses are presented in Tables 2-6. Total iron was determined as FeO. Fe_2O_3 in case of chromites was calculated based on spinel stoichiometry. The characteristic features of the rocks are described following the cumulate terminology of Wager et al. (1960).

The olivine cumulate is a mesocumulate consisting of a subhedral olivine framework (Fig. 4) with interstitial post-cumulus orthopyroxene. Olivine is pseudomorphed by serpentine. Pale brown, faintly pleochroic bronzitic orthopyroxene is a post-cumulus phase. Large, irregular oikocrysts of orthopyroxene poikilitically enclose olivine

Fig.4. Olivine-orthopyroxene cumulate, Bondla complex, Goa.

forming a heteradcumulate. Up-section the modal proportion of pyroxene increases to enable classification of the rock as peridotite. The layers exhibit igneous lamination (e.g. Wager and Brown, 1967) defined by preferred alignment of the longer axis of olivine crystals in the plane of layering. Peridotite is overlain by a massive chromitite horizon which shows heteradcumulate texture made up of large irregular chromites that appear to have grown by sintering of chromites. Such chromites poikilitically enclose rounded and vermicular silicates (occluded silicate texture) represented by pseudomorphs of serpentine after olivine. Elsewhere chromite is subhedral and forms a mosaic within which vermicular and rounded silicates are enclosed forming net- and chain- texture (Fig. 5). Chromite is faintly anisotropic and shows higher reflectivity along borders due to alteration to ferritchromit (e.g. Spangenberg, 1943; Bliss and McLean, 1975; Jan et al. 1985) Chromite shows exsolutions of ilmenite (Fig.6) parallel to (111) due to sub-solidus re-equilibration.

The complex displays well developed cryptic layering which is best displayed by the rocks of the Upper Zone. In the Lower Zone it could be studied only in chromites and rarely in orthopyroxenes as the rocks are altered and relict phases except for chromite and orthopyroxene are rarely available. The Cr# [Cr/(Cr+Al)] jumps from 0.63-0.64 (Mg# [Mg/(Mg+Fe^{+2})] 0.51) in chromites from dunites to 0.81-0.96 (Mg#: 0.06-0.11) for those in chromitites above them (Table 2). The latter are less aluminous (1-7 wt % Al_2O_3) than those (>17 wt % Al_2O_3) in peridotites. Further up-section Cr# in chromites from troctolite decreases to 0.66-0.69 (Mg#: 0.36-0.42; 12-13 wt% Al_2O_3). This abrupt decrease in Cr# from chromitite chromites to troctolite chromites is indicative of reversal in cryptic variation. The compositional variation exhibited by chromites is depicted in Fig. 7.

TiO_2 in all analysed chromites is >0.5 wt% and Al_2O_3 is greater than MgO. These features are characteristic of ores

Table 2. Composition of chrome spinels from the Bondla mafic-ultramafic complex

Sr. No	1	2	3	4	5	6	7	8	9
Smp. No	B19A	B19A	B19A	B15	B15	B15	BT1	BT1	BT1
TiO_2	0.72	0.75	0.78	0.51	0.72	0.7	3.35	3.37	3.45
Al_2O_3	17.02	17.15	17.17	1.58	1.36	1.38	13.26	13.25	12.87
Cr_2O_3	45.17	45.19	45.19	54.92	52.05	54.25	41.1	39.59	38.01
Fe_2O_3	8.99	8.99	8.54	12.45	15.29	13.04	14.39	16.19	17.79
FeO	17.32	17.12	17.46	27.09	27.2	27.45	20.1	19.2	20.74
MgO	10.41	10.46	10.52	1.43	1.45	1.09	7.25	7.89	6.66
MnO	0.33	0.3	0.3	1.98	1.91	2.06	0.51	0.47	0.44
Total	99.96	99.96	99.96	99.96	99.98	99.97	99.96	99.96	99.96
Cations recalculated on the basis of 32 oxygens									
Ti	0.14	0.14	0.15	0.11	0.16	0.15	0.66	0.66	0.69
Al	5.12	5.15	5.16	0.54	0.47	0.48	4.1	4.09	4.01
Cr	9.13	9.12	9.13	12.7	12.1	12.6	8.56	8.22	7.97
Fe^{+3}	1.73	1.73	1.64	2.68	3.38	2.88	2.85	3.2	3.55
Fe^{+2}	3.7	3.66	3.73	6.64	6.68	6.75	4.43	4.22	4.6
Mg	3.97	3.98	4.01	0.62	0.63	0.48	2.85	3.09	2.63
Mn	0.07	0.06	0.06	0.49	0.46	0.51	0.11	0.1	0.1
Cr#	0.64	0.63	0.63	0.95	0.96	0.96	0.67	0.66	0.66
Fe^{+3}#	0.1	0.1	0.1	0.16	0.21	0.18	0.18	0.2	0.22
Mg#	0.51	0.52	0.51	0.08	0.08	0.06	0.39	0.42	0.36

1-3: Peridotites, 4-6: Chromitites, 7-9: Troctolites

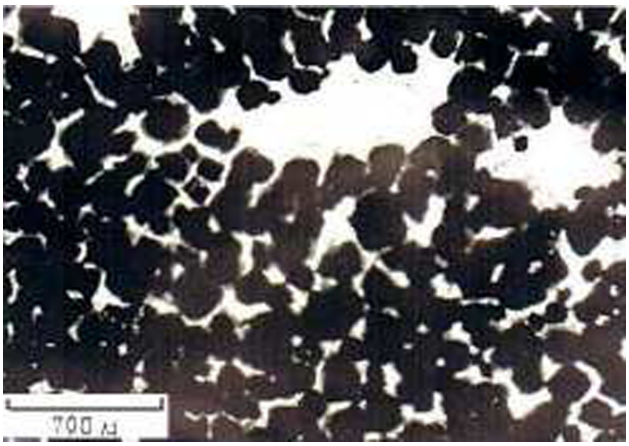

Fig.5. Net- and chain-texture in chromitite from Bondla complex.

from layered intrusions. Dessai et al. (1995b) classify these ores as of stratiform-type. Chromites compositionally similar, from some late Archaean complexes show decrease in Cr/Fe ratios and increase in iron and titanium e.g. those from the Mashaba (2900 Ma) and Stillwater (2700Ma) complexes. These are considered to have been emplaced in unstable continental environments and are categorized as Archaean greenstone-hosted chromites (e.g. Leblanc, 1985; Stowe, 1994).

The Upper Zone begins with a thin impersistent horizon of pyroxenites and consists largely of pyroxene and plagioclase cumulates. Up-section the lower part of this zone comprises olivine-plagioclase cumulates (troctolites). Gabbroic rocks further up-section containing >15 vol% orthopyroxene and <50 vol% plagioclase in the mode are here referred to as gabbronorites whereas those containing >50 vol% plagioclase are classified as leucogabbros. The gabbroic rocks thus vary from troctolites to gabbronorites that make up the bulk of this zone with leucogabbros at the top. The troctolite is an adcumulate of olivine (Fo_{85-86}, Table 3) and plagioclase (Table 4) in which the percentage

Fig.6. Exsolutions of ilmenite in chromite from Bondla.

of post-cumulus plagioclase is insignificant. The gabbronorites are mesocumulates in the lower part of the section and contain pyroxene and plagioclase both as the framework and post-cumulus constituents. Up-section they exhibit orthocumulate texture which is also seen in the overlying leucogabbros. Both clinopyroxene and plagioclase are strongly zoned with irregular corroded cores overgrown by optically discontinuous mantles. The leucogabbros at the extreme top of the intrusion exhibit granophyric texture. The compositional variation shown by the minerals with stratigraphic height is presented in Fig. 8. This zone in general exhibits uniform layering. In certain sections e.g. the one NE of Ganje size-graded layering can be distinguished. The bottom of the layer is generally coarser grained (1-2 cm cpx, >3 cm plg.) gradually becoming finer grained towards the top. In the section at Durgini the gabbros overall exhibit uniform layering. At places, however, layers with a more melanocratic base are seen and they are rarely size graded.. Such mineral- and size-graded layers are, however, limited to certain sections that have restricted lateral continuity.

The rocks of the Upper Zone display cryptic variation that is more conspicuous here than in the zone below. Most mineral phases that show distinct and systematic variation in composition from bottom to top can be best described with reference to the framework silicates and post cumulus phases. In the pyroxene quadrilateral the Ca-poor pyroxenes

Table 3. Composition of olivines from the Bondla mafic-utramafic complex

Sr. No	1	2	3	4	5	6
Smp No	BT1	BT1	BT1	BT1	BT1	BT1
SiO_2	40.37	40.08	40.07	40.4	40.53	40.39
TiO_2	0.02	0.01	0.01	0.01	0.01	0.01
Al_2O_3	0	0.01	0.01	0	0.01	0
Cr_2O_3	0.06	0.03	0.02	0.02	0.01	0.03
FeO	13.46	13.37	13.43	13.13	13.25	13.25
MnO	0.17	0.18	0.18	0.16	0.17	0.15
MgO	45.75	46.16	46.09	46.13	45.83	45.97
CaO	0.12	0.11	0.13	0.1	0.12	0.14
Total	**99.95**	**99.95**	**99.94**	**99.95**	**99.93**	**99.94**
Cations recalculated on the basis of 4 oxygens						
Si	1.004	0.9954	991	1.0033	1.0067	1.0037
Ti	0.0002	0.0001	0.0001	0	0.0001	0
Al	0	0.0007	0.0001	0	0.0001	0
Cr	0.001	0	0.0003	0	0.0002	0.0004
Fe	0.0281	0.286	0.2805	0.2736	0.2762	0.2763
Mg	1.7017	1.7146	1.7164	1.7134	1.7025	1.7085
Mn	0.0034	0.0037	0.0037	0.0032	0.0035	0.0031
Fo	86	85	86	86	86	86

Analyses 1-6 : Troctolite

Table 4. Composition of plagioclases from the Bondla mafic-utramafic complex

Sr No	1	2	3	4	5	6	7	8	9	10	11	12	13	14	15	16
Smp No.	BT1	BT1	BT1	BT1	GB1 C	GB1 C	GB1 R	GB1 R	GB1 PC	GB1 PC	GB2 C	GB2 R	GB2 R	GB2 R	GB2 R	GB2R
SiO_2	46.78	46.81	46.98	46.86	47.44	53.4	55.73	57.72	64.31	65.82	54.49	59.24	54.63	56.2	56.06	57.34
TiO_2	0.04	0.02	0.01	0.02	0	0.06	0.05	0.06	0.02	0	0.03	0.04	0.07	0.04	0.05	0.05
Al_2O_3	33.58	33.54	33.21	33.4	32.95	28.29	27.29	26.28	22.9	21.67	28.06	25.58	27.47	27.89	26.78	26.26
Cr_2O_3	n.a.	n.a.	n.a.	n.a.	n.a.	n.a.	n.a.	n.a.	n.a.	n.a.	n.a.	n.a.	n.a.	n.a.	n.a.	n.a.
FeO	0.39	0.34	0.41	0.4	0.4	0.69	0.8	0.64	0.09	0.1	0.8	0.66	0.78	0.8	0.83	0.64
MnO	0.02	0	0	0	0.02	0.04	0.01	0.01	0	0.02	0.01	0.05	0.01	0.11	0.02	0.06
MgO	0.07	0.1	0.09	0.08	0.13	0.1	0.17	0.05	0.02	0.01	0.12	0.01	0.11	0.11	0.08	0.04
CaO	17.85	17.66	17.63	17.54	17.21	12.19	11.39	9.52	3	2.44	12.15	8.27	11.34	11.5	10.67	9.29
Na_2O	1.35	1.38	1.36	1.35	1.77	4.19	4.5	5.72	8.97	9.62	4.47	6.28	4.76	4.95	5.24	5.79
K_2O	0.01	0.02	0.03	0.02	0.06	0.26	0.3	0.38	0.67	0.3	0.21	0.41	0.24	0.31	0.34	0.33
Total	**100.09**	**99.87**	**99.72**	**99.67**	**99.98**	**99.22**	**100.24**	**100.38**	**99.98**	**99.98**	**100.34**	**100.54**	**99.41**	**101.91**	**100.07**	**99.8**
Cations recalculated on the basis of 8 oxygens																
Si	2.1506	2.1541	2.1654	2.1608	2.1791	2.4402	2.5024	2.5872	2.8323	2.8889	2.4617	2.6378	2.4863	2.4969	2.5307	2.5815
Ti	0.0011	0.0005	0.0002	0.0005	0	0.0019	0.0016	0.0018	0.0005	0	0.0008	0.001	0.0021	0.0008	0.0016	0.0016
Al	1.8218	1.8213	1.8213	1.8174	1.786	1.5256	1.4589	1.3898	1.19	1.1222	1.4959	1.3438	1.5452	1.462	1.4265	1.3948
Fe+2	0.0149	0.013	0.0158	0.0152	0.0152	0.0264	0.0303	0.024	0.0031	0.0034	0.0302	0.0244	0.0296	0.0294	0.0313	0.0241
Mg	0.0047	0.0066	0.0061	0.0052	0.0088	0.0066	0.0114	0.0032	0.001	0.0005	0.0079	0.0005	0.0074	0.0065	0.0051	0.0024
Ca	0.8822	0.8736	0.8737	0.8694	0.8498	0.5988	0.5546	0.5486	0.1418	0.1151	0.5901	0.3957	0.5546	0.5491	0.5178	0.4495
Na	0.1206	0.1234	0.1217	0.1209	0.1578	0.3723	0.3964	0.4986	0.7682	0.8213	0.3925	0.5437	0.4212	0.427	0.46	0.5068
K	0.0005	0.0011	0.0016	0.0011	0.0033	0.0151	0.0084	0.0216	0.0377	0.0166	0.0119	0.0233	0.0137	0.0172	0.0196	0.019
Mn	0.0005				0.0077	0.0013	0.0002	0.0002		0.0005	0.0002	0.0018	0.0002	0.0038	0.0005	0.0021
An mole%	87	87	87	87	84	60	57	51	15	12	59	41	56	55	52	46
Ab mole%	12	12	12	12	15	37	41	47	84	86	40	56	42	43	47	52
Or mole%	<1	<1	<1	<1	1	1	2	1	1	1	1	2	1	1	1	1

Table.4 continued

Sr No	17	18	19	20	21	22	23	24	25	26	27	28	29	30	31
Smp No.	GB2 PC	GS23 C	GS23 C	GS23 C	GS23 C	GS23 C	GS23 R	GS23 R	GS23 R	GD12C	GD12C	GD12C	GD12R	GD12 PC	GD12 PC
SiO_2	59.97	52.04	51.87	57.35	52.84	53.53	54.42	54.77	56.96	55.01	58.13	58.28	60.89	62.12	62.72
TiO_2	0	0.06	0.03	0.09	0.05	0.05	0.04	0.06	0.04	0.07	0.09	0.04	0.01	0.06	0.06
Al_2O_3	22.76	29.89	30.24	26.15	29.32	28.73	28.19	28.39	26.76	27.53	25.65	25.26	24.34	22.92	22.9
Cr_2O_3	n.a.	n.a.	n.a.	n.a.	n.a.	n.a.	n.a.	n.a.	n.a.	n.a.	n.a.	n.a.	n.a.	n.a.	n.a.
FeO	0	0.49	0.46	0.5	0.43	0.58	0.28	0.31	0.4	0.61	0.56	0.61	0.31	0.42	0.44
MnO	0.06	0	0	0.05	0.01	0	0.01	0	0.08	0	0.01	0	0.02	0	0.02
MgO	0.06	0.03	0.04	0.08	0.03	0.05	0.03	0.02	0.02	0.08	0.07	0.03	0.02	0.02	0.01
CaO	4.51	13.34	1353	9.44	12.89	12.44	11.2	11.13	9.53	11.26	8.91	8.09	6.58	5.25	5.17
Na_2O	8.09	3.85	3.57	5.59	3.91	4.29	4.79	4.91	5.56	4.85	5.99	6.29	7.33	7.81	8.07
K_2O	4.51	0.27	0.24	0.47	0.31	0.3	0.32	0.38	0.62	0.35	0.57	0.65	0.47	0.72	0.54
Total	**99.96**	**99.97**	**1439.5**	**99.72**	**99.79**	**99.97**	**99.28**	**99.97**	**99.97**	**99.76**	**99.98**	**99.25**	**99.97**	**99.32**	**99.93**
Cations recalculated on the basis of 8 oxygens															
Si	2.7265	2.3677	2.3587	2.5835	2.4256	2.4295	2.474	2.4733	2.5627	1.8697	2.6127	2.6326	2.7111	2.7768	2.7844
Ti	0	0.0019	0.0008	0.0029	0.0016	0.0016	0.001	0.0019	0.001	0.0016	0.0029	0.001	0.0002	0.0018	0.0018
Al	1.2211	1.6047	1.6226	1.3901	1.5882	1.5386	1.5122	1.5128	1.4205	1.1041	1.3597	1.3464	1.2789	1.209	1.1996
Fe+2	0	0.0186	0.0175	0.0187	0.0163	0.0218	0.0104	0.0117	0.0149	0.0172	0.0208	0.0228	0.0115	0.0156	0.0163
Mg	0.0038	0.0019	0.0024	0.0051	0.0019	0.0032	0.0019	0.001	0.001	0.0038	0.0046	0.0019	0.001	0.001	0.0005
Ca	0.2204	0.6524	0.6614	0.4572	0.6361	0.6067	0.5472	0.5403	0.4609	0.4111	0.4249	0.3927	0.3149	0.252	0.2465
Na	0.7152	0.1701	0.3156	0.2447	0.349	0.3785	0.4235	0.4311	0.4864	0.3205	0.5236	0.5524	0.6347	0.679	0.6968
K	0.2623	0.0104	0.0137	0.0133	0.0179	0.0172	0.0183	0.0217	0.0355	0.0151	0.0327	0.0375	0.0265	0.0204	0.0305
Mn	0.0021	0	0	0.0019	0.0005	0	0.0002	0	0.0029	0	0.0002	0	0.0005	0	0.0005
An mole%	18	78	66	64	63	60	55	54	47	55	43	40	32	26	25
Ab mole%	81	20	32	34	34	38	42	44	49	42	55	56	65	70	71
Or mole%	1	1	1	1	1	2	2	2	3	1	1	3	2	3	3

Analyses: 1-4: Troctolites 5-25: gabbronorites 26-31 Leucogabbros; C:Core R: Rim PC: Post-cumulus

Table 5. Composition of clinopyroxenes from the Bondla mafic-utramafic complex

Sr. No	1	2	3	4	5	6	7	8	9	10	11	12	13	14	15	16	17	18
Smp No	B19A	B19A	B19A	N1	N1	B4	B4	B4	B4	BT1	BT1	BT1	BT1	GB1 R	GB1 PC	GB1 PC	GB1 R	GB1PC
SiO_2	53.87	53.52	53.68	53.27	53.21	55.08	54.89	53.94	53.49	55.56	54.41	53.67	53.25	52.28	49.02	48.97	50.38	49.17
TiO_2	0.22	0.2	0.24	0.25	0.23	0.01	0.02	0.04	0.05	0.3	0.2	0.21	0.43	0.41	0.59	0.65	0.61	0.58
Al_2O_3	2.81	2.2	2.22	2.24	2.22	1.67	0.16	0.18	0.74	1.67	1.6	1.97	2.1	2.37	1.22	1.39	2.29	1.19
Cr_2O_3	1	0.98	0.99	0.91	0.97	0.77	0.01	0.07	0.01	0.77	0.66	0.74	0.84	0.03	0.01	0.01	0.01	-
FeO	4.07	3.88	3.95	4.32	4.28	2.9	3.21	4.33	4.46	0.37	3.77	3.96	4.11	15.6	27.08	26.49	15.92	27.16
MnO	0.15	0.14	0.09	0.14	0.09	0	0.16	0.15	0.14	0.17	0.17	0.13	0.13	0.33	0.57	0.56	0.37	0.52
MgO	16.83	16.91	16.81	17.25	17.12	13.35	16.51	17.66	16.85	18.43	17.77	18.1	18.1	17.96	7.53	8.07	13.81	7.98
CaO	21.41	21.62	21.67	21.27	21.61	25.04	25.25	22.37	24.04	22.45	21.91	21.73	21.73	10.76	13.79	13.58	15.76	13.53
Na_2O	0.23	0.25	0.26	0.26	0.24	0.01	0.21	0.01	0.14	0.22	0.21	0.19	0.19	0.14	0.16	0.01	0.27	0.2
K_2O	0					0	0	0	0	0.01	0.01		0.01	-49.02	0.01		0	
Total	**100.59**	**99.7**	**99.91**	**99.91**	**99.97**	**98.83**	**100.42**	**98.75**	**99.92**	**99.95**	**100.71**	**100.7**	**100.89**	**50.86**	**99.98**	**99.73**	**99.42**	**100.33**
Cations recalculated on the basis of 6 oxygens																		
Si	1.9581	1.9517	1.9532	1.9419	1.934	2.0119	1.9974	1.9767	1.9813	1.9793	1.9423	1.9344	1.9139	1.8904	1.9592	1.9453	1.9222	1.9523
Ti	0.0059	0.0052	0.0063	0.0068	0.0061	0.0002	0.0004	0.0008	0.0013	0.0079	0.0052	0.0056	0.0114	0.0111	0.0175	0.0184	0.0174	0.0172
Al^{IV*}	0.044	0.041	0.038	0.055	0.057	0.000	0.004	0.008	0.032	0.000	0.033	0.062	0.079	0.051	0.046	0.048	0.051	0.046
Al^{VI}	0.077	0.054	0.058	0.041	0.038	0.074	0.003	0.000	0.000	0.071	0.035	0.022	0.010	0.053	0.011	0.018	0.053	0.011
Cr	0.0287	0.0285	0.0285	0.027	0.276	0.0003	0.0019	0	0	0.0216	0.0187	0.0211	0.0024	0.0006	0.0002	0.0002	0.0002	0
Fe^{+2}	0.124	0.1204	0.1204	0.1312	0.1304	0.0887	0.0978	0.1334	0.1387	0.0219	0.1139	0.12	0.1239	0.4668	0.9047	0.8829	0.5096	0.905
Mn	0.0046	0.0041	0.0026	0.0041	0.0048	0	0.0048	0.0041	0.0042	0.0049	0.005	0.0039	0.0054	0.01	0.0192	0.0186	0.0119	0.0174
Mg	0.9149	0.9198	0.9147	0.9404	0.963	0.8931	0.8984	9676	0.9355	9818	0.9584	0.9777	1.0014	0.9712	0.4485	0.4793	0.7879	0.4683
Ca	0.8366	0.8475	0.8476	0.8335	0.8282	0.9832	9877	0.8812	0.9571	0.8598	0.8494	0.8437	0.8362	0.5818	0.5873	0.5914	0.6462	0.5775
Na	0.0081	0.0175	0.0182	0.0182	0.0168		0.0006	0.0148	0.0006	0.015	0.0145	0.0132	0.0151	0.0098	0.0122	0.0007	0.02	0.0153
K			0.0004							0.0004	0.0004		0.0004		0.0004			
Wo	44.6	44.93	44.92	43.73	43.09	50.03	49.78	44.45	47.16	46.13	44.2	43.45	42.63	28.8	30.26	30.27	33.24	29.59
En	48.78	48.76	48.48	49.33	50.11	45.45	45.28	48.81	46	52.68	49.87	50.36	51.05	48.08	23.11	24.53	40.53	24
Fe	6.61	6.29	6.38	6.93	6.78	4.5	4.92	6.72	6.83	1.1	5.92	6.18	6.77	23.11	46.62	45.19	26.21	46.39
Mg#	0.88	0.88	0.88	0.87	0.88	0.9	0.9	0.87	0.87	0.97	0.89	0.89	0.88	0.67	0.33	0.35	0.6	0.34

Table5. Contd….

Sr. No	19	20	21	22	23	24	25	26	27	28	29	30	31	32	33	34	35	36
Smp No	GB2 C	GB2 C	GB2 C	GB2 PC	GB2 PC	GB2 PC	GB2 PC	GS23 C	GS23 C	GS23 C	GS23 C	GS23 R	GS23 R	GD12C	GD12C	GD12R	GD12R	GD12R
SiO_2	52.69	52.64	51.87	50.44	49.78	49.98	51.03	52.24	51.87	52.42	51.5	51.41	53.74	52.04	52.13	50.68	51.15	53.05
TiO_2	0.29	0.27	0.48	0.61	0.71	0.52	0.12	0.28	0.31	0.46	0.39	0.55	0.37	0.56	0.58	0.87	0.8	0.87
Al_2O_3	2.58	3.13	2.49	1.66	2	1.44	0.99	2.65	2.5	1.9	2.63	1.93	2.91	2.08	2.05	1.79	1.8	1.56
Cr_2O_3	0.32	0.18	-	-	-	0.03	-	0.13	0.17	0.08	0.1	0.06	-	0.17	0.04	-	0.02	0.03
FeO	8.02	8.41	12.51	23.09	21.8	25.31	26.37	7.56	7.41	8.74	9.12	9.97	14.74	11.94	13.32	17.09	17.58	22.88
MnO	0.15	0.2	0.29	0.41	0.4	0.52	0.3	0.2	0.21	0.3	0.24	0.26	0.38	0.27	0.29	0.32	0.36	0.26
MgO	18.54	17.93	16.49	12.93	10.75	9.64	6.29	16.23	15.59	14.87	15.22	14.18	16.21	15.37	14.98	12.09	12.45	8.74
CaO	17.14	16.76	15.55	10.6	14.25	13.07	14.68	20.22	21.51	20.87	19.8	20.47	10.84	17.1	16.81	16.83	16.43	12.39
Na_2O	0.18	0.27	0.24	0.2	0.21	0.2	0.16	0.29	0.29	0.3	0.31	0.31	0.6	0.25	0.25	0.02	0.33	0.13
K_2O	-	-	-	-	0.01	-	0.02	-		0.08	0.01	-	0.17	0	0	0	0.01	0.05
Total	**99.91**	**99.79**	**99.92**	**99.94**	**99.91**	**100.71**	**99.96**	**99.8**	**99.86**	**100.02**	**99.32**	**99.14**	**99.96**	**99.78**	**100.45**	**99.69**	**100.93**	**99.96**
Cations recalculated on the basis of 6 oxygens																		
Si	1.9279	1.9304	1.9299	1.9474	1.9352	1.9511	2.0179	1.9284	1.9205	1.9467	1.9233	1.9365	1.9847	1.9408	1.9434	1.9412	1.9372	2.0453
Ti	0.0079	0.0072	0.0132	0.0176	0.0205	0.015	0.0003	0.0075	0.0084	0.0127	0.0108	0.0154	0.0102	0.0155	0.0164	0.0249	0.0226	0.0251
Al^{IV*}	0.052	0.084	0.052	0.073	0.056	0.080	0.067	0.000	0.054	0.055	0.053	0.064	0.000	0.0541	0.0552	0.0526	0.0645	0.0000
Al^{VI}	0.013	0.019	0.004	0.038	0.027	0.035	0.019	0.128	0.038	0.035	0.028	0.016	0.072	0.0375	0.0349	0.0285	0.0158	0.0724
Cr	0.0092	0.003	0	0	0	0.0007	0	0.0037	0.0049	0.0022	0.0029	0.0015	0	0.0494	0.0011	0	0.0004	0.0002
Fe^{+2}	0.2462	0.2587	0.3906	0.7483	0.7104	0.8293	0.8751	0.2341	0.2302	0.2723	0.286	0.3152	0.4567	0.3435	0.4167	5492	0.5586	0.7207
Mn	0.0171	0.0061	0.0089	0.0132	0.0131	0.0171	0.01	0.0062	0.0064	0.0094	0.0074	0.0081	0.0115	0.0085	0.0089	0.0103	0.0114	0.0083
Mg	1.0145	0.9779	0.9175	0.7464	0.6238	0.5626	0.372	0.896	0.8632	0.8257	0.8499	0.7986	0.8952	0.8573	0.8651	0.6923	0.705	0.5038
Ca	0.6741	0.6607	0.622	0.4398	0.5943	0.5485	0.624	0.8022	0.856	0.853	0.795	0.8289	4302	6854	0.6735	0.6929	0.6689	0.5133
Na	0.0127	0.0192	0.0172	0.0149	0.0156	0.015	0.0121	0.027	0.0207	0.0214	0.0225	0.0227	0.0429	0.0174	0.0179	0.0013	0.0242	0.0095
K													0.008				0.0004	0.0023
Wo	34.84	34.82	32.22	22.73	30.81	28.26	33.34	41.51	43.9	43.8	41.7	42.66	24.14	35.76	34.98	35.81	34.61	29.08
En	52.43	51.54	47.53	38.58	32.34	28.99	19.88	46.36	44.27	42.7	44.01	41.1	50.23	44.73	43.37	35.79	36	28.53
Fe	12.72	13.37	20.23	38.68	36.83	42.73	46.76	12.11	11.8	14.11	14.11	16.22	25.62	19.58	21.64	28.38	48	42.39
Mg#	0.8	0.79	0.7	0.49	0.46	0.4	0.29	0.79	0.78	0.75	0.74	0.71	0.66	0.69	0.66	0.55	28.9	0.41

1-5: Peridotites, 6-9: Pyroxenites; 10-13: Troctolites; 14-25: Gabbros; 26-31: Gabbronorites; 32-36: Leucogabbros

* Clinopyroxenes have Si+Al<2 and the shortfall is compensated by Ti and Fe^{3+}

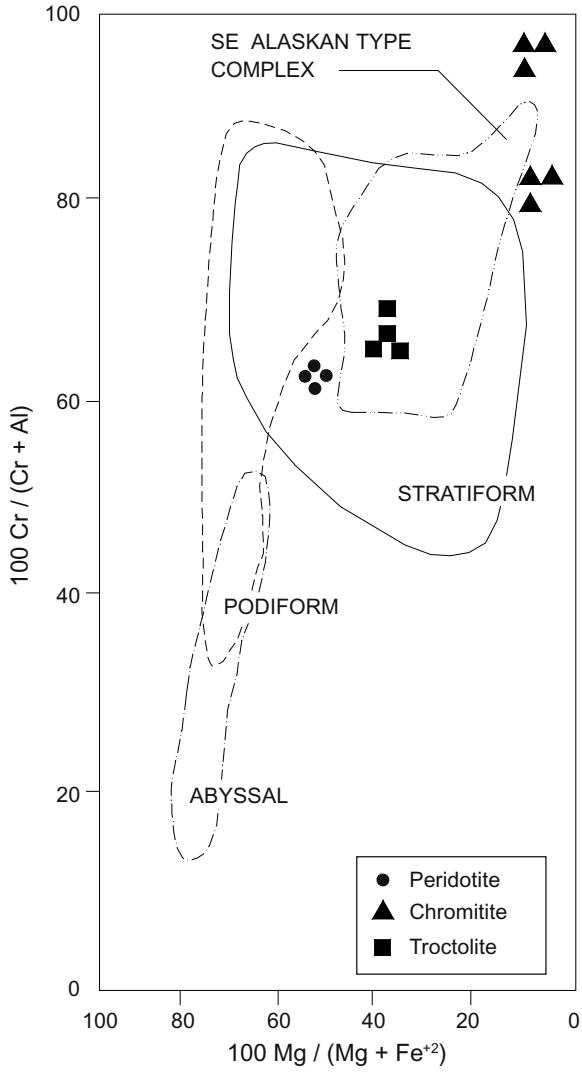

Fig. 7. Cr # versus Mg # plot depicting the compositions of chromites from the Bondla complex.

plot in the enstatite field (Fig. 9). The majority of the Ca-rich pyroxenes can be classified as augites and a few as sub-calcic augites. The clinopyroxenes from the troctolites coexist with enstatite as shown by the tie lines. Clinopyroxene ($Wo_{50-44}En_{45-48}Fs_{4-6}$) in pyroxenites is a subcalcic-augite with Mg# varying from 0.87-0.90 (Table 5). In the overlying troctolite the clinopyroxene ($Wo_{42-46}En_{51-52}Fs_{6-1}$) is represented by augite with higher Mg # varying from 0.89-0.97. This is a case of reversal in cryptic variation. Orthopyroxene ($Wo_{2-4}En_{85-82}Fs_{12}$) in troctolite is represented by bronzite/enstatite with a restricted variation in Mg# (0.86-0.87) (Table 6). In the overlying gabbronorites, orthopyroxene shows a larger variation ($Wo_{4-2}En_{60-84}Fs_{34-12,}$ Mg #: 64-0.87) and can be characterised as pigeonite. Clinopyroxene shows distinct zoning unlike that in the troctolite. Core compositions are typically ($Wo_{32-41}En_{52-44}Fs_{12-15,}$ Mg#:0.70-0.80) more magnesian than the rim ($Wo_{24-42}En_{50-41}Fs_{25-16}$; Mg# 0.66-0.71) which is more ferrian. Post-cumulus clinopyroxene ($Wo_{30-22}En_{23-38}Fs_{46-38}$; Mg #: 0.33-0.49) is much more ferrian in comparison to the pyroxenes described above and can be classified as ferroaugite. In the overlying leucogabbros the composition of clinopyroxene core is $Wo_{34-35}En_{43-44}Fs_{21-19}$ (Mg#: 0.66-0.69). The rim composition is similar to the composition of the post-cumulus pyroxene in the underlying gabbro-norites. The pyroxenes in general show a distinct and progressive trend towards iron enrichment across the intrusion and particularly so those from the upper zone (Fig. 10).

Ubiquitous plagioclase is the other important phase present throughout the upper zone. Bytownite (An_{87}) is the dominant composition in the troctolites and in the gabbronorites the composition of the cores varies from labradorite to bytownite (An_{60-84}). The composition of plagioclase cores (An_{55-63}) in the lecogabbros is similar to that of the plagioclase rims (An_{51-57}) in the gabbronorites. Though the post-cumulus plagioclase in the entire section shows a compositional variation from $An_{10-40,}$ the variation within and between the lithohorizons is considerable. Like the pyroxenes, the plagioclases from the upper zone show a systematic and progressive change towards more albitic compositions from the bottom to the top. Core to rim and rim to post-cumulus distinctions as well as interrelationships are depicted by the evolutionary trend (Fig.11).

WHOLE ROCK GEOCHEMISTRY

Representative least altered samples of the selected lithotypes were analyzed for major element by x-ray fluorescence spectroscopy on fused glass discs, at NGRI, Hyderabad. Analytical precision was assessed by measurement of natural and synthetic standards. Total iron was determined as FeO. Ferric iron was calculated following Le Maitre (1976). Rare earth elements and several other trace elements were analyzed by Inductively Coupled Plasma Mass Spectroscopy (ICP-MS) at NGRI. USGS standards were used to calibrate the ICP-MS results. Precision is estimated to be 2-4% of the reported value. All analyses are processed on an anhydrous basis.

Major Elements

Major oxide analyses of 13 samples are presented in Table 7. The range of SiO_2 in ultramafic rocks is 43-44 wt% except for one sample of a pyroxenite which has 52 wt% SiO_2. In the mafic rocks SiO_2 varies from 49-52 wt%. TiO_2

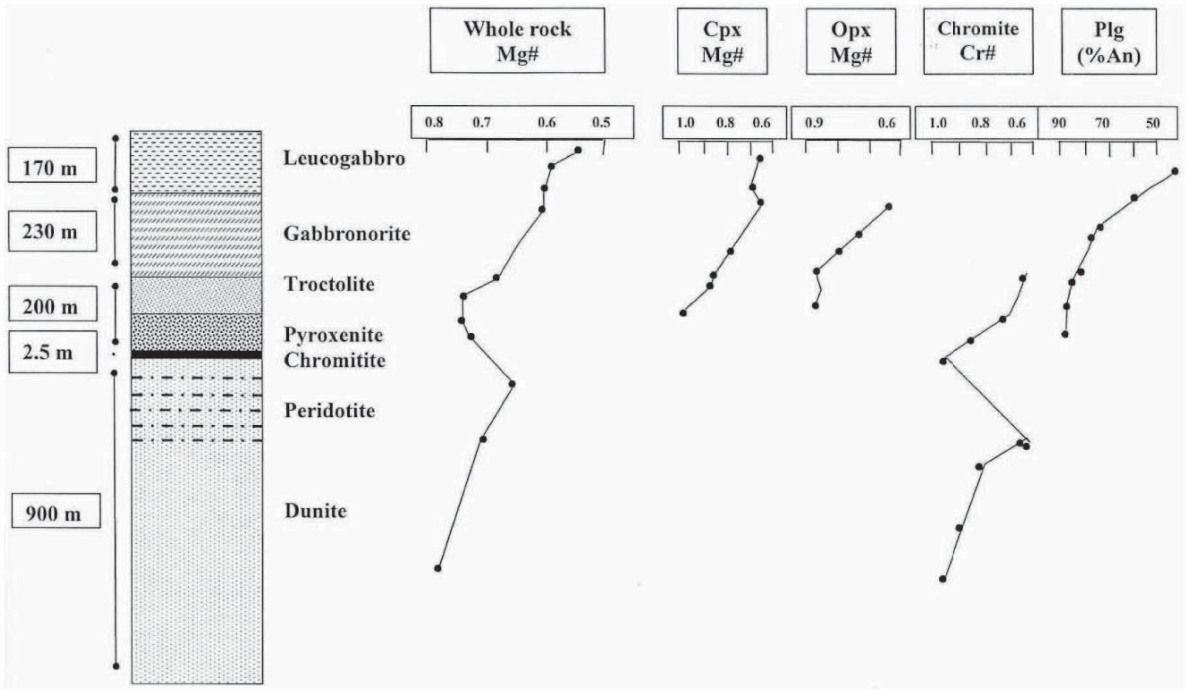

Fig.8. Litholog of the Bondla mafic-ultramafic complex showing the compositional variation of minerals with stratigraphic height.

in all rocks and particularly in the gabbroic ones is less than 0.8 wt% and thus the rocks can be classified as low-Ti gabbroids. Mg # (Mg/Mg + Fe^{+2}) varies from 0.74-0.58. The ultramafic rocks contain >35 wt% MgO, while in the gabbroic rocks MgO varies from 9-12 wt%. It must be emphasized that these variations have limited value in characterizing the magma-type, the rocks being cumulates. However, selectively and with a note of caution some elemental variations could be utilized to understand the evolutionary process. Most of the gabbros are quartz normative but few are olivine normative. Inter element variations e.g., TiO_2, Al_2O_3, Fe_2O_3 and CaO show positive correlation with Mg# whereas SiO_2 and FeO show an inverse correlation (Fig. 12).

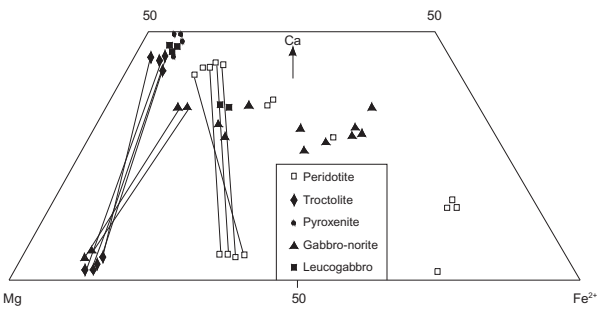

Fig.9. Compositions of pyroxenes from the Bondla complex in the pyroxene quadrilateral. Tie-lines connect clino-pyroxenes and orthopyroxenes from the same rock type.

Trace Elements

Trace element concentrations of 8 samples are presented in Table 7. Large ion lithophile elements (LILE) are plotted against Zr (Fig. 13) as it is relatively more incompatible in gabbroic assemblage (Faure, 1992). Ba, Rb, Sr and REE show positive correlation whereas Cr, Ni and V show large variation between samples and exhibit negative correlation with Zr. Positive correlation indicates their incompatibility whereas negative correlation suggests compatibility with the fractionating phases. Representative MORB normalized (e.g. Saunders and Tarney, 1984; Sun, 1980) trace element patterns are presented in Fig. 14. The patterns of the

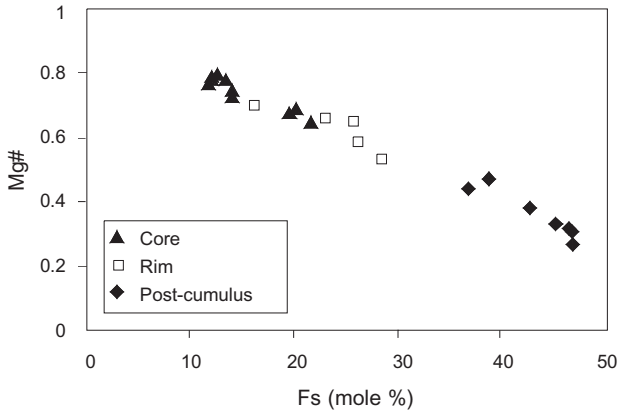

Fig.10. Mg# versus Fs (mole %) plot depicting the compositional variations in pyroxenes with advancing crystallization.

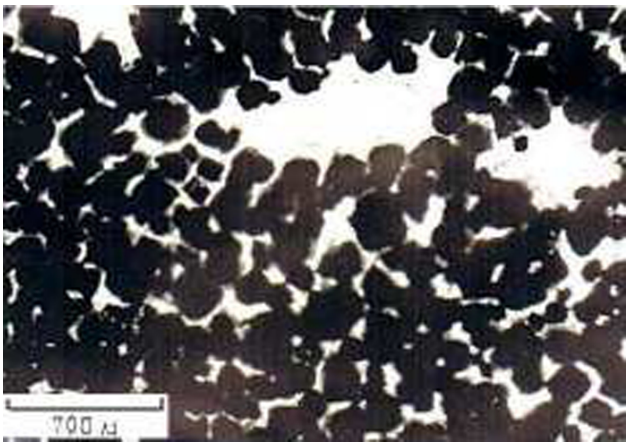

Fig.5. Net- and chain-texture in chromitite from Bondla complex.

from layered intrusions. Dessai et al. (1995b) classify these ores as of stratiform-type. Chromites compositionally similar, from some late Archaean complexes show decrease in Cr/Fe ratios and increase in iron and titanium e.g. those from the Mashaba (2900 Ma) and Stillwater (2700Ma) complexes. These are considered to have been emplaced in unstable continental environments and are categorized as Archaean greenstone-hosted chromites (e.g. Leblanc, 1985; Stowe, 1994).

The Upper Zone begins with a thin impersistent horizon of pyroxenites and consists largely of pyroxene and plagioclase cumulates. Up-section the lower part of this zone comprises olivine-plagioclase cumulates (troctolites). Gabbroic rocks further up-section containing >15 vol% orthopyroxene and <50 vol% plagioclase in the mode are here referred to as gabbronorites whereas those containing >50 vol% plagioclase are classified as leucogabbros. The gabbroic rocks thus vary from troctolites to gabbronorites that make up the bulk of this zone with leucogabbros at the top. The troctolite is an adcumulate of olivine (Fo_{85-86}, Table 3) and plagioclase (Table 4) in which the percentage

Fig.6. Exsolutions of ilmenite in chromite from Bondla.

of post-cumulus plagioclase is insignificant. The gabbronorites are mesocumulates in the lower part of the section and contain pyroxene and plagioclase both as the framework and post-cumulus constituents. Up-section they exhibit orthocumulate texture which is also seen in the overlying leucogabbros. Both clinopyroxene and plagioclase are strongly zoned with irregular corroded cores overgrown by optically discontinuous mantles. The leucogabbros at the extreme top of the intrusion exhibit granophyric texture. The compositional variation shown by the minerals with stratigraphic height is presented in Fig. 8. This zone in general exhibits uniform layering. In certain sections e.g. the one NE of Ganje size-graded layering can be distinguished. The bottom of the layer is generally coarser grained (1-2 cm cpx, >3 cm plg.) gradually becoming finer grained towards the top. In the section at Durgini the gabbros overall exhibit uniform layering. At places, however, layers with a more melanocratic base are seen and they are rarely size graded.. Such mineral- and size-graded layers are, however, limited to certain sections that have restricted lateral continuity.

The rocks of the Upper Zone display cryptic variation that is more conspicuous here than in the zone below. Most mineral phases that show distinct and systematic variation in composition from bottom to top can be best described with reference to the framework silicates and post cumulus phases. In the pyroxene quadrilateral the Ca-poor pyroxenes

Table 3. Composition of olivines from the Bondla mafic-utramafic complex

Sr. No	1	2	3	4	5	6
Smp No	BT1	BT1	BT1	BT1	BT1	BT1
SiO_2	40.37	40.08	40.07	40.4	40.53	40.39
TiO_2	0.02	0.01	0.01	0.01	0.01	0.01
Al_2O_3	0	0.01	0.01	0	0.01	0
Cr_2O_3	0.06	0.03	0.02	0.02	0.01	0.03
FeO	13.46	13.37	13.43	13.13	13.25	13.25
MnO	0.17	0.18	0.18	0.16	0.17	0.15
MgO	45.75	46.16	46.09	46.13	45.83	45.97
CaO	0.12	0.11	0.13	0.1	0.12	0.14
Total	**99.95**	**99.95**	**99.94**	**99.95**	**99.93**	**99.94**
Cations recalculated on the basis of 4 oxygens						
Si	1.004	0.9954	991	1.0033	1.0067	1.0037
Ti	0.0002	0.0001	0.0001	0	0.0001	0
Al	0	0.0007	0.0001	0	0.0001	0
Cr	0.001	0	0.0003	0	0.0002	0.0004
Fe	0.0281	0.286	0.2805	0.2736	0.2762	0.2763
Mg	1.7017	1.7146	1.7164	1.7134	1.7025	1.7085
Mn	0.0034	0.0037	0.0037	0.0032	0.0035	0.0031
Fo	86	85	86	86	86	86

Analyses 1-6 : Troctolite

Table 7. Major (wt%) and trace (ppm) element compositions of mafic and ultramafic rocks from Bondla

Sr. No.	1	2	3	4	5	6	7	8	9	10	11	12	13
Smp. No.	B19A	G11	N1	B4	BT1	BT2	GB1	GB2	GS23	S35	S36	GD12	BT3
SiO_2	43.35	44.56	42.77	52.5	51.65	50.74	51.41	49.61	50.37	52.27	51.81	49.28	50.47
TiO_2	0.03	0.11	0.14	0.61	0.82	0.77	0.72	0.64	0.63	0.7	0.65	0.64	0.59
Al_2O_3	2.59	2.82	2.80	19.15	20.42	20.98	19.00	18.82	19.31	16.43	17.96	17.86	16.69
Fe_2O_3	1.57	1.66	1.64	2.34	2.48	2.42	2.44	2.26	2.22	2.44	2.36	2.25	2.25
FeO	9.38	10.85	13.89	1.54	1.28	1.32	1.08	2.17	2.78	2.36	3.13	3.97	3.99
MnO	0.25	0.13	0.27	0.06	0.07	0.07	0.08	0.11	0.23	0.12	0.12	0.15	0.18
MgO	40.46	38.89	36.47	12.24	12.56	12.53	9.05	9.84	9.43	9.80	9.66	11.08	9.27
CaO	2.25	0.82	1.24	11.35	9.87	10.13	14.87	15.19	13.86	14.46	12.96	13.54	15.22
Na_2O	0.01	0.01	0.02	0.06	0.69	0.55	1.00	0.99	0.85	1.06	1.01	0.92	1.10
K_2O	0.03	0.06	0.01	0.08	0.05	0.38	0.22	0.23	0.19	0.22	0.21	0.18	0.21
P_2O_5	0.05	0.05	0.05	0.05	0.07	0.07	0.08	0.08	0.08	0.07	0.08	0.06	0.07
Total	**99.97**	**99.96**	**99.3**	**99.98**	**99.96**	**99.96**	**99.95**	**99.94**	**99.95**	**99.93**	**99.95**	**99.93**	**100.04**
Mg #	0.74	0.7	0.64	0.72	0.73	0.73	0.68	0.64	0.6	0.62	0.58	0.58	0.54
Trace elements (ppm)													
V	648		166	648		128		169	197	159		156	
Cr	11426		1227	11426		372		188	244	261		172	
Ni	217		373	217		129		96	90	78		82	
Cu	11		105	11		28		132	106	72		104	
Ga	21		7	22		10		19	18	14		17	
Ba	11		14	11		35		34	35	81		37	
Rb	6		2	6		15		11	10	6		8	
Sr	3		15	3		99		274	237	218		225	
Y	2		5	2		2		11	11	11		10	
Zr	4		4	4		6		28	26	33		26	
Nb	<1		1	0.51		<1		2	1	0		2	
Th	<1		<1	0.44		<1		<1	<1	0		<1	
U	<1		<1	0.28		<1		<1	<1	0		<1	
Hf	1		2	0.94		<1		3	3	n.a.		2	
Ta	<1		<1	0.2		1		1	<1	n.a.		<1	
La	1		1	1.64		2		3	2	4		3	
Ce	<1		1	1		1		5	5	12		6	
Nd	1		2	1.6		2		5	5	6		5	
Sm	2		3	2.1		2		3	3	1		3	
Eu	<1		<1	0.42		<1		1	1	<1		1	
Gd	1		2	1.13		2		3	3	n.a.		3	
Tb	n.a.		n.a.	0.4		n.a.		n.a.	n.a.	0.5		n.a.	
Dy	<1		2	0.88		1		4	3	n.a.		2	
Er	<1		1	0.7		1		2	2	n.a.		1	
Yb	1		1	0.62		<1		3	3	1		2	
Lu	0.8		<1	0.2		<1		1	1	1		<1	
Ti	180		840	3662		23		3843	3843	4203		3843	
K	249		83	664		26		1909	1494	1826		1494	
P	218		218	218		305		349	262	305		262	

Analyses 1-3:peridotites 4: pyroxenite 5-6:troctolites 7-9:gabbronorites 10-13: leucogabbros;n.a.: not analysed

cumulates (Fo_{85-86}) crystallised from a liquid with Mg# between 0.72 and 0.73. Thus the troctolite (BT1) with wholerock Mg# 0.73 may represent the most primitive magma. It is characterized by Cr > 400 ppm, Ni ~ 370 ppm and SiO_2 between 50-51 wt percent. These values are within the ranges generally accepted for primitive magmas (Rhodes, 1981) except that Ni values are slightly lower. Further low-TiO_2 and low alkali contents are consistent with its sub-alkaline nature.

The complete spectrum of rocks from ultrabasic to leucogabbroic types observed at Bondla Complex depicts the evolution of the magma from the early to late stages of differentiation. The observed sequence of crystallization at Bondla is spinel + olivine + pyroxene + plagioclase. Spinel (Cr-Al) and olivine are cotectic phases of tholeiitic magmas. Pyroxene compositions also enable characterization of the magma type. The presence of Ca-rich and Ca-poor pyroxenes each with exsolutions of the other, their evolution towards

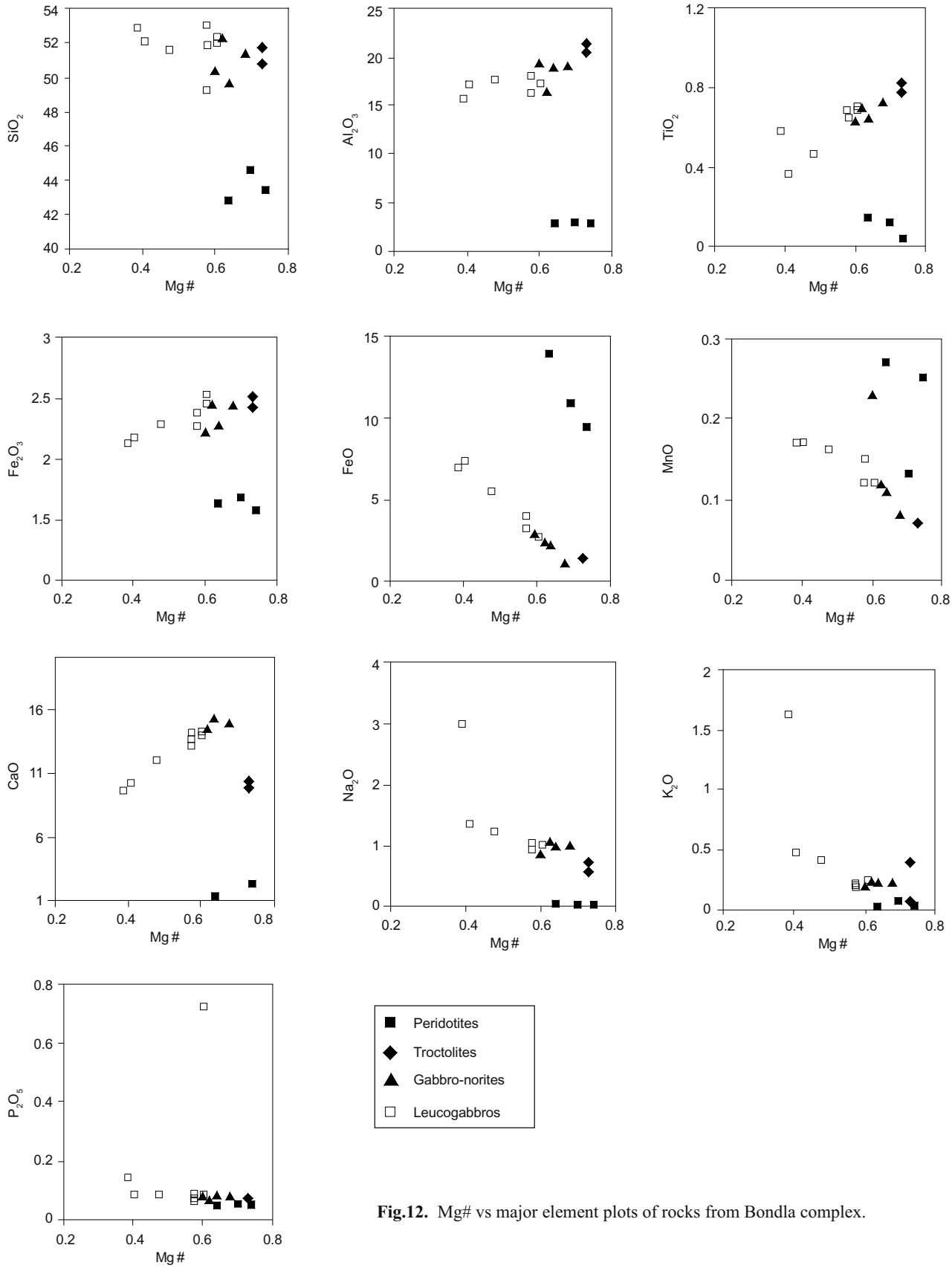

Fig.12. Mg# vs major element plots of rocks from Bondla complex.

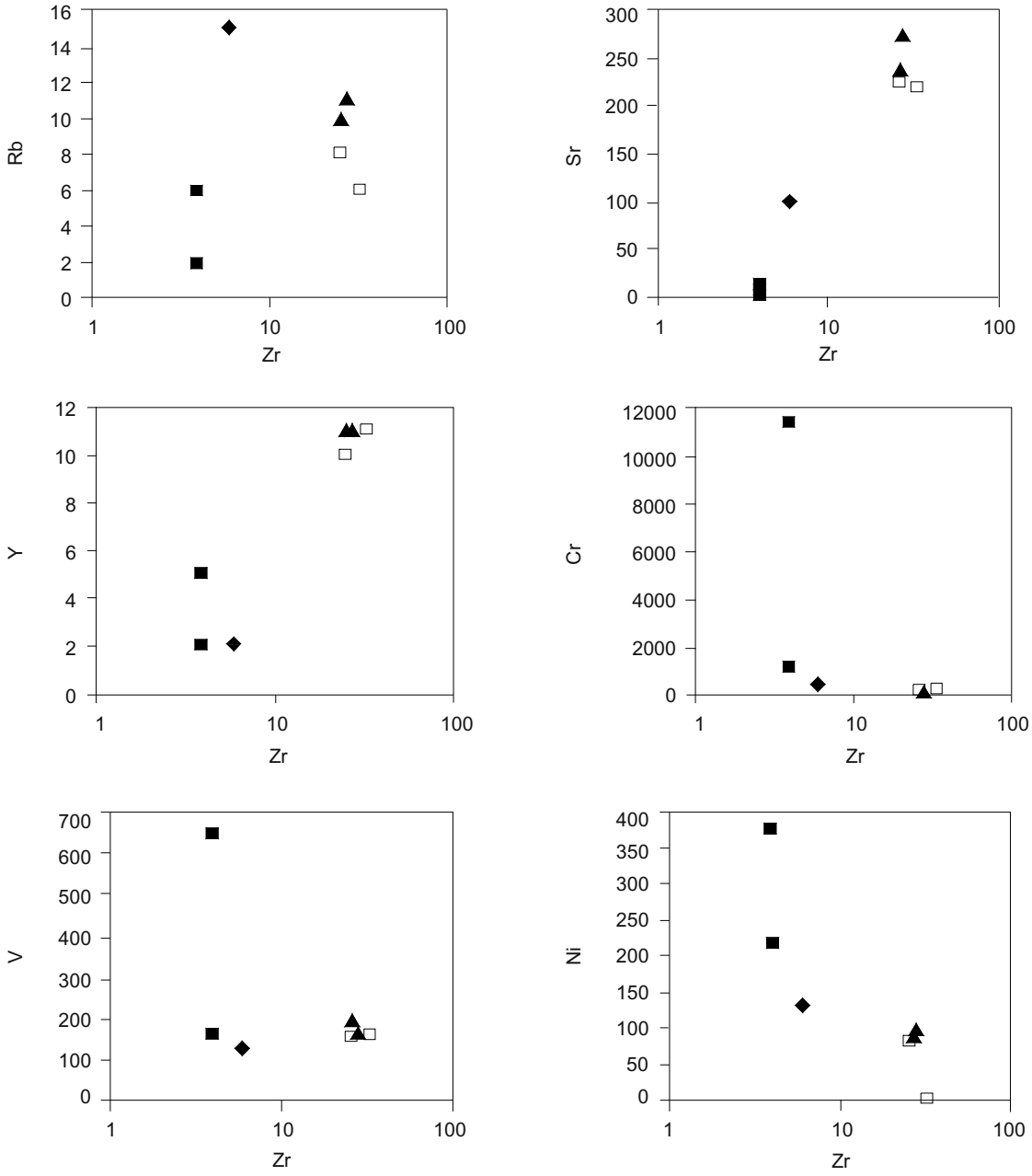

Fig.13. Zr vs trace element plots of rocks from Bondla complex. Symbols same as in Fig.12.

iron-rich compositions and co-existence with olivine (e.g. Deer et al. 1997) is indicative of a tholeiitic magma type. Progressive iron enrichment observed in successive differentiation products is a feature characteristic of tholeiitic differentiation (Wager and Brown, 1967; Kuno, 1968). This is evident from the evolution of pyroxene towards ferrian composition in stratigraphically higher rocks as depicted in Fig. 9. For example the magnesian augite and pigeonite from the troctolites progressively change to ferroaugite and ferropigeonite in the gabbronorites (ferrogabbros) and leucogabbros of the Upper Zone providing evidence of their tholeiitic lineage. This is supported by the low concentration of alumina in the tetrahedral site (Al_z) of pyroxene. Further evidence of an iron-enriched trend during the course of crystallisation is provided by the observed lithological variation. For example, the troctolites of the Upper Zone give way to ferrogabbros (here referred to as gabbronorites) higher up in the section. This is apparent from the AFM plot (Fig. 15) of whole rock analyses that show a distinct trend towards iron-rich compositions of successive daughter

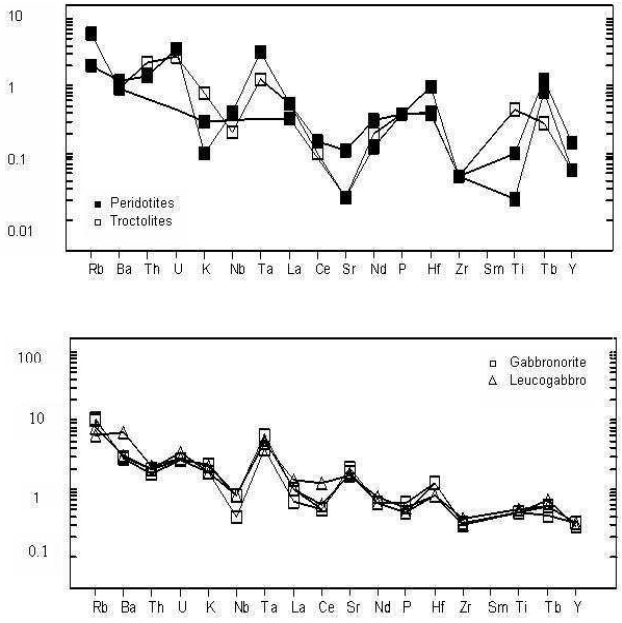

Fig.14. Multielement spiderdiagram of rocks from Bondla complex.

magmas characteristic of the differentiation of a tholeiitic magma. The trend is more iron-rich compared to a typical tholeiite but less than that displayed by the Skaergaard intrusion (Wager and Brown, 1967) which illustrates the extreme case of iron-enrichment. This trend is normally accompanied by higher silica content in the differentiates. The quartz-normative compositions of the rock suite confirm

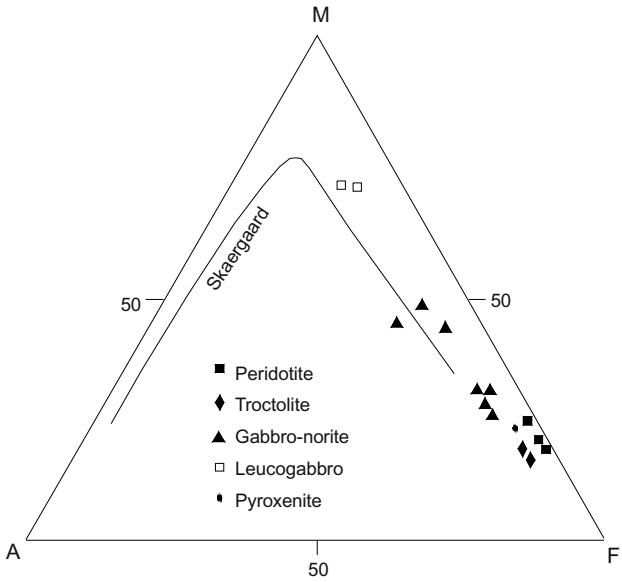

Fig.15. AFM plot depicting progressive compositional variation of rocks from Bondla Complex (*after* Wager and Brown, 1967; Kuno, 1968).

that the magma evolved from the tholeiitic side of the thermal barrier. However, the mafic rocks contain higher alumina (> 17 wt %: Al_2O_3) suggesting that they may have been the products of a high-alumina basalt magma-type. In the present case, however, the higher alumina content of the rocks is due to the accumulation of plagioclase and hence is not an inherent characteristic of the magma-type. It is pertinent to note here that as a rule high-iron rocks are always more alumina-rich than are typical Fe-basalts (e.g. Pearce and Birkett, 1974) whereas high-alumina rocks have more iron than typical high-alumina basalts (Kuno, 1969).

Magmatic Differentiation

The whole rock chemical data can provide useful information on the course of differentiation/ magmatic evolution. The major part of the intrusion is characterized by a gabbroic mineral assemblage with olivine as an important phase in the early stages and clinopyroxene and plagioclase in the latter stages. The increase in CaO and Al_2O_3 (Fig. 12) in the initial stages of crystallization supports olivine dominated fractionation whereas their further decrease indicates pyroxene and plagioclase crystallisation. Clinopyroxene controlled fractionation is also evident from the decrease of CaO/Al_2O_3 ratio and the positive trend shown by Rb, Sr and REE with Zr. Decrease of V in the initial stages (from peridotite to troctolite) and its increase in the later stages along with that of Ti (from troctolite to leucogabbros) suggests that precipitation of Fe-Ti oxides decreased during the later stages of differentiation. The gabbroic nature of the mineral assemblage has resulted in the formation of large amounts of pyroxene-rich cumulates and gabbronorites as seen so conspicuously at Bondla.

The positive relationship between Mg# versus Cr and Ni is consistent with early fractionation of olivine and chromite from the initial magma pulse possibly driving the magma to silica saturation that stabilised Ca-poor pyroxene in preference to Ca-rich pyroxene. The other possibility that could be ascribed to the stabilization of Ca-poor pyroxene is the elevated SiO_2 in the magma (e.g. Campbell, 1985; Barnes, 1989) as a result of crustal assimilation. Contamination by assimilation of crustal rocks finds support in the coexistence of Ca-rich (augite) and Ca-poor (pigeonite) pyroxenes and the Nb/La ratio which is a useful index of crustal contamination. Continental basaltic magmas typically show Nb/La values between 0.14 and 1.4 (Thomson et al. 1984). The Bondla rocks in particular show values between 0.4 and 0.6 suggesting that the magma may have undergone significant crustal contamination. It is also supported by a positive correlation between Ba/Nb and SiO_2

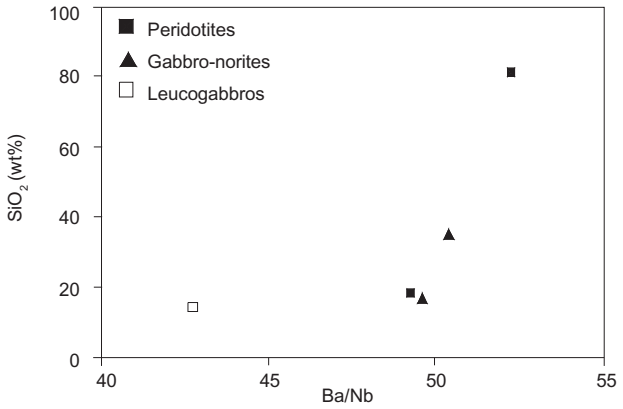

Fig.16. Ba/Nb versus SiO_2 variations in rocks from Bondla complex.

(Fig.16). This latter possibility seems to be more likely in the present case.

Magma Mixing in a Replenished Magma Chamber

Both the lower and upper zones of the Bondla Complex are characterized by a specific mineral assemblage that displays a distinctive imprint of the compositional variation that the magma has been subjected to during the course of crystallization. This is evident from the normal-reverse-normal cryptic variation exhibited by the mineral phases from the bottom to the top of the intrusion (Fig.8). This similarity in behaviour supports the hypothesis that the two zones which are physically separated represent two magma sub-chambers. The chromitite-pyroxenite marker that is sandwiched between the two zones is suggestive of the interconnected nature of the two sub-chambers.

The Lower Zone rocks contain Ca-poor pyroxene that continues up to the pyroxenite horizon. The presence of Ca-poor pyroxene indicates the anhydrous nature of the magma which prevailed until the crystallization of pyroxenites. However, subsequent to the formation of pyroxenites, an increase in the water content of the magma is apparent and is evident from the stabilization of olivine which leads to the formation of troctolites.

The bytownitic nature of the troctolite plagioclase (An_{84}) gives credence to the presence of water in the magma at this stage (e.g. Helz, 1973). Higher Mg #s (0.97-0.88) of clinopyroxenes from the pyroxenites and troctolites than those (0.90-0.87) from peridotites suggests a reversal of cryptic variation. This can be attributed to incomplete magma mixing, occurring, as a result of the replenishment of the resident magma in the chamber by a more primitive magma pulse. Copious precipitation of chromites at this stage of evolution may indicate that the newly injected pulse of magma may have been at the threshold of chromite crystallization. The drop in temperature as a result of magma mingling led to excessive precipitation of chromite that almost impoverished the magma in chromium, so much so that the rocks that crystallized subsequently were almost devoid of chromites. Further, the dominance of clinopyroxene in the later rocks prevented crystallization of chromites as an independent phase, as the former can accommodate significant amounts of Cr in its structure.

Rhythmic layering and normal – reverse – normal cryptic variation coupled with the association of a variety of cumulate lithologies suggests that the crystallization in the north-western sub chamber was of an open-system-type characterized by periodic replenishment by more primitive melts. This process of repeated injection of magma pulses may have occurred in the early stages of magma chamber formation. The pyroxenite – chromitite horizon possibly

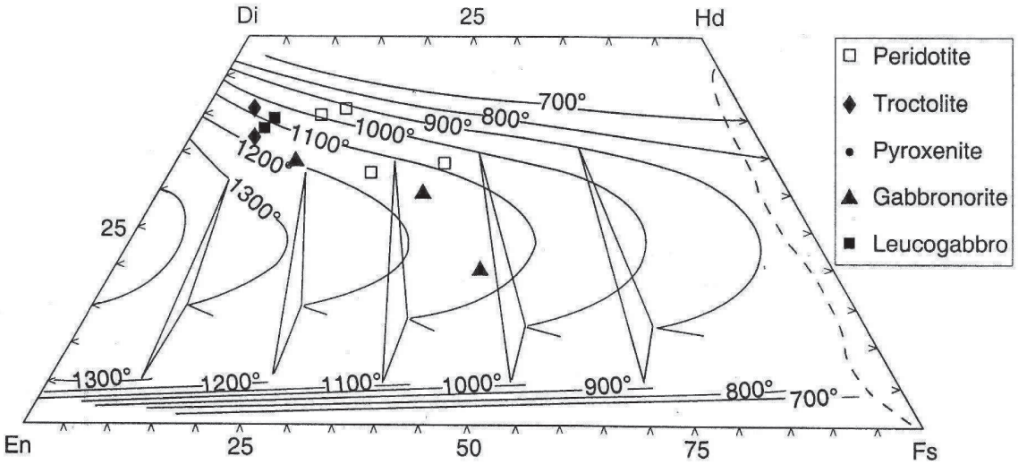

Fig.17. Plots of pyroxene compositions from the Bondla complex in the experimentally contoured Ca-Mg-Fe phase relations diagram at 1.0 GPa (*after* Lindsley, 1983).

marks the end of this process of magma integration. Subsequent crystallization of gabbros of the Upper Zone was largely a result of differentiation of the last magma pulse.

Temperature and Depth of Crystallization

A quantitative assessment of the temperature of crystallization was made using the empirical geothermometers of Lindsley (1983). Ca-rich pyroxenes from the most primitive troctolite (BT1) indicate a temperature range from 1150-1200°C at 1.0GPa (Fig. 17). Clinopyroxenes from gabbronorites (GB1, GS23), provide values of 1100-1150°C, whereas those from the stratigraphically higher leucogabbros (e.g. GS23) yield temperatures of about 1000°C. This temperature range is substantiated by petrographic evidence which indicates that gabbroic rocks crystallized very close to the inversion temperature of pigeonite with Mg # varying from 0.60-0.63. Orthopyroxenes with Mg #s in the range of 0.60-0.63 correspond to a crystallization temperature of 1100°C (e.g. Barnes and Hoatson, 1994). Similarly olivine with Fo_{89} could have a melt temperature of about 1350 °C (e.g. Ballhaus and Glikson, 1989). The Bondla troctolite, the most primitive rock of the suite, has olivine with Fo_{86}. Hence it may be suggested that the range of temperatures of primitive melts at Bondla may have been approximately 1200-1300°C which broadly corresponds with the petrographically estimated ranges of temperatures for similar rocks from other parts of the world.

A tentative estimate of prevalent pressures can be made from the fractionated minerals. Dominance of olivine and chromite in the northwestern sub-chamber is suggestive of equilibration pressures of more than 1.0 GPa, whereas the predominance of plagioclase in the southeastern sub-chamber is indicative of pressures below 1.0 GPa. The low pressure origin of plagioclase is also supported by the low mole % K (0.3) in it (e.g. Ai and Green, 1989). This tentative pressure range is relevant in the context of magma generation and subsequent crystallisation. Low-Ti basaltic melts normally originate at pressures of less than 1.0 GPa (e.g. Sun and Nesbitt, 1978). It can be surmised that the depth of magma generation and the depth of crystallization of Bondla complex were similar.

CONCLUSIONS

The Bondla mafic-ultramafic complex is a layered intrusion that consists of ultramafic and mafic cumulates. It is divisible into two zones on the basis of the chromitite-pyroxenite-troctolite marker horizon which displays distinct reversal in cryptic variation. The lower zone is rhythmically layered and consists of olivine-chromite and olivine+ pyroxene-chromite cumulates. The chromite layers exhibit way up stratigraphy and alternate with layers of olivine± pyroxene. The top of this zone is marked by a massive chromitite layer which is overlain by the pyroxenites and troctolites. The upper zone commences with troctolites at the base which are followed by gabbronorites (ferrogabbros) and leucogabbros at the top. It exhibits uniform layering which is characterized by regular normal cryptic variation seen in pyroxenes and plagioclases along the entire section of this zone.

The complex has resulted from intrusion of a low-TiO_2 sub-alkaline tholeiitic magma that may have been modified by fractional crystallization, and periodic injection of a more primitive chrome-rich magma into the pre-existing magma chamber. Field relations suggest that the complex evolved in a magma chamber that consisted of two interconnected sub-chambers as evident from the existence of a chromite-pyroxenite marker horizon at the site of both the subchambers.

Acknowledgements: We thank Goa University for financial and logistic support. Thanks are also due to Energy Technology, CSIRO, NSW, Australia for EPMA data.

References

Ai, Y. and Green, D.H. (1989) Phase relations in the system anorthite-potassium feldspar at 10 kb with emphasis on their solid solution. Miner. Mag., v.53, pp.337-345.

Alapieti, T.T., Halkoaho, T.A.A., Deavraju, T.C. and Jayaraj, K.R. (1994) Chromite hosted PGE mineralization in the Channagiri area, Karnataka state, India. Proc. VII International Platinum Symposium, Moscow, pp.3-4 (Abstract).

Balakrishnan, S, Abbas, M.H., Vidyadharan, K.T. and Raghunandan, K.R. (1992) Chromite and sulphide mineralization in the mafic-ultramafic complex of Usgao, Goa, Indian Minerals, v.41, pp.303-322.

Ballhaus, C.G. and Glikson, A.Y. (1989) Magma mixing and intraplutonic quenching in the Wingelina Hills intrusion, Giles complex, Central Australia. Jour. Petrol., v.30, pp.1443-1469.

Barnes, S.J. (1989) Are Bushveld U-type parent magmas boninites or contaminated komatiites? Contrib. Mineral. Petrol., v.101, pp.447-457.

Barnes, S.J. and Hoatson, D.M. (1994) The Munni Munni Complex, western Australia: stratigraphy, structure and petrogenesis. Jour. Petrol., v.35, pp.715-751.

Bliss, N.J. and McLean, W.H. (1975) The paragenesis of zoned

chromites from Manitoba. Geochim. Cosmochim. Acta, v.39, pp.973-990.

Campbell, I. H. (1985) The differences between oceanic and continental tholeiites: a fluid dynamic explanation. Contrib. Mineral. Petrol., v.91, pp.37-43.

DeBari, S.M. (1964) Petrogenesis of the Fiambala gabbroic intrusion, northwestern Argentina, a deep crustal syntectonic pluton in a continental magmatic arc. Jour. Etrol. v.35, pp.679-713.

Deer, W.A., Howie, R.A. and Zussman, J. (1997) Rock forming minerals, Single-chain Silicates. Geol. Soc. London, v.2A, 668p.

Dessai, A.G. and Peshwa, V.V. (1982) Manganese mineralization in a tropical forest area, Goa, India: A study based on aerial photographs and Landsat-1 imagery interpretation. *In:* D.J.C.Haming, and A. K. Gibbs (Eds.), Hidden Wealth: Mineral Exploration Techniques in tropical forest areas, pp.170-175.

Dessai, A.G., French, D. and Arolkar, D.B. (1994) Mineralogy of polymetallic sulphide mineralization in Archaean greenstones at Tisk-Usgao, Goa, India. Curr. Sci., v.66, pp.824-825.

Dessai, A.G., Arolkar, D.B. and French, D. (1995a) Cu-Ni sulphide mineralization in greenstones at Tisk-Usgao, Goa. Jour. Indian Assoc. Sedimentologists, v.14, pp.1-18.

Dessai, A.G., French, D. and Arolkar, D.B. (1995b) Geochemistry of stratiform chromites from the Bondla mafic-ultramafic complex, Usgao, Goa, India. Jour. Indian Assoc. Sedimentologists, v.15, pp.17-29.

Devaraju, T.C., Alapieti, T.T., Halkoaho, T.A.A., Jayaraj, K.R. and Khanadali, S.D (1994) Evidence of PGE mineralization in the Channagiri mafic Complex, Shimoga district, Karnataka. Jour. Geol. Soc. India, v.43, pp.317-318.

Dhoundial, D. P., Paul, D. K., Sarkar, A., Trivedi, J. R., Gopalan, K. and Potts, P.J. (1987) Geochronology and geochemistry of Precambrian granitic rocks of Goa, southwest, India. Precambrian Res., v.36, pp287-302.

Faure, G. (1992) Principles and applications of inorganic geochemistry. Macmillan Publishing Company, New York, 626p.

Gokul, A.R. (1985) Structure and tectonics of Goa. Earth Resources for Goa's development. Goa Seminar Volume, Geol. Surv. India, pp.14-21

Gokul, A.R. and Srinivasan, M.D. (1976) Chandranath Granite, Goa. Rec. Geol. Surv. India, v.107, pp.38-45.

Green, T.H. and Pearson, N.J. (1987) An experimental study of Nb and Ta partitioning between Ti-rich minerals and silicate liquids at high pressure and temperature. Geochim Cosmochim Acta, v.51, pp.55-62.

Helz, R.T. (1973) Phase relations of basalts in their melting range at P_{H_2O} = 5 Kb as a function of oxygen fugacity: Part I Mafic phases. Jour. Petrol., v.14, pp.249-302.

Jan, M.F., Windley, B.F. and Khan, A.A. (1985) The Waziristan ophiolite, general geology and chemistry of chromites and associated phases. Econ. Geol., v.80, pp.249-306.

Kuno, H. (1968) Differentiation of basalt magmas, *In:* H.H. Hess and A. Poldervaart (Eds.), Basalts; Poldervaart treatise on rocks of basaltic composition. Interscience, John Wiley and Sons, New York, pp.623-688.

Kuno, H. (1969) Plateau basalts. In: Hart, P. (Ed.) The earth's crust and upper mantle. Amer. Geophys. Union, Geophysics Monograph, v.13, pp.495-501.

Leblanc, M. (1985) Les gisements de spinelles chromiferes. Bull. Mineral, v.108, pp.587-602

Le Maitre, R.W. (1976) The chemical variability of some common igneous rocks. Jour. Petrol., v.17, pp.589-637.

Lindsley, D.H. (1983) Pyroxene thermometry. Amer. Mineral., v.68, pp.477-493.

Pearce, T.H. and Birkett, T.C. (1974) Archaean metavolcanic rocks from Thackeray township, Ontario. Can. Mineral., v.12, pp.509-519.

Rhodes, J.M. (1981) Characteristics of primary basalt magmas. *In:* Basaltic Volcanism on the terrestrial planets. Pergamon, Oxford, pp.409-452.

Saunders, A.D. and Tarney, J (1984) Goechemical characteristics of basaltic volcanism within back-arc basins. *In:* B.P. Kokelar and M. F. Howells (Eds.), Marginal basin geology: volcanic and associated sedimentary and tectonic processes in modern and ancient marginal basins. Geol. Soc. London Spec. Publ., pp.59-76.

Serri, G. (1981) Petrochemistry of ophiolite gabbroic complexes: a key for the classification of ophiolites into low-Ti and High-Ti types. Earth Planet. Sci. Lett., v.51, pp.203-212

Spangenberg, K. (1943) Die Chromitlager statte von Jampadal am Zobten E: Zeitschr. Parakt, Geologie, v.5, pp.13-35.

Stowe, C.W. (1994) Compositions and tectonic settings of chromite deposits through time. Econ. Geol., v.89, pp.528-546.

Sun, S. S. (1980) Lead isotope study of young volcanic rocks from mid-oceanic ridges and island-arcs. Phil. Trans. Royal. Soc. London, v.A297, pp.409-445

Sun, S.S. and Nesbitt, R.W. (1978) Petrogenesis of Archaean ultrabasic volcanics from the rare earth elements. Contrib. Mineral. Petrol., v.65, 301p.

Thomson, R.N., Hendry, G.L. and Parry, S.J. (1984) An assessment of the relative roles of the crust and mantle in magma genesis: an elemental approach. Phil. Trans. Royal Soc. London, v.A310, pp.549-590

Vidyadharan, K.T. and Palaniappan, K. (2006) Mafic – ultramafic and related rocks of Southern Indian shield – potential target areas for PGE mineralization. Jour. Applied Geochemistry, v.8, pp.475-500.

Wager, L.R. and Brown, G.M. (1967) Layered Igneous Rocks. W. H. Freeman & Co., Olliver and Boyd, Edinburg, London, 588p.

Wager, L.R., Brown, G.M. and Wadsworth, W.J. (1960) Types of igneous cumulates. Jour. Petrol., v.73, pp.73-85.

(Received: 13 August 2007; Revised form accepted: 22 December 2008)